X-ray diffraction and Raman spectroscopic studies on supercooled and glassy aqueous zinc(II) iodide solutions

ARTICLE *in* THE JOURNAL OF PHYSICAL CHEMISTRY · NOVEMBER 1991

Impact Factor: 2.78 · DOI: 10.1021/j100177a087

3 AUTHORS:

Toshiyuki Takamuku
Saga University
84 PUBLICATIONS **1,933** CITATIONS
SEE PROFILE

Toshio Yamaguchi
Fukuoka University
204 PUBLICATIONS **3,867** CITATIONS
SEE PROFILE

Hisanobu Wakita
Fukuoka University
151 PUBLICATIONS **1,680** CITATIONS
SEE PROFILE

X-ray Diffraction and Raman Spectroscopic Studies on Supercooled and Glassy Aqueous Zinc(II) Iodide Solutions

Toshiyuki Takamuku,† Toshio Yamaguchi,* and Hisanobu Wakita

Department of Chemistry, Faculty of Science, Fukuoka University, Nanakuma, Jonan-ku, Fukuoka 814-01, Japan *(Received: April 12, 1991; In Final Form: July 10, 1991)*

X-ray diffraction and Raman spectral measurements have been performed on aqueous zinc(II) iodide solutions with the $[H_2O]/[ZnI_2]$ molar ratios of 5 and 10 in ambient temperature and the supercooled liquids and the glassy state. The X-ray radial distribution functions show that in the ambient temperature and supercooled solutions an average coordination number of iodide ions for a zinc(II) ion is about 2 and does not change significantly with temperature, while the number of nonbonding I···I interactions per zinc(II) ion within the zinc(II) iodo complexes increases from 2.0 at room temperature to 2.4 in the supercooled state. Raman bands for the symmetric Zn–I stretching vibration (ν_1) of the diiodo-, triiodo-, and tetraiodo zinc(II) complexes are separately observed for the solutions in the three states; with decreasing temperature the ν_1 band for the diiodo complex decreases in intensity but that for the tetraiodo complex increases. A broad Raman band for the symmetric Zn–O stretching vibration (ν_1) of the aqua zinc(II) ion is also observed, and the band intensity increases with decreasing temperature. These results suggest that the following disproportionation reaction (eq 1) occurs in the supercooled and glassy solutions: $2[ZnI_2(OH_2)_2] + 2H_2O \rightarrow [ZnI_4]^{2-} + [Zn(OH_2)_6]^{2+}$. This shift in equilibrium is discussed on the basis of enhanced hydrogen bonds between water molecules in the supercooled and glassy solutions.

Introduction

Supercooled and glassy solutions have long been used in radiation chemistry such as Mössbauer, ESR, and ESCA studies of reaction intermediates and coordination species in solutions[1] and in cryobiology for conservation of biological materials in solutions.[2,3] Moreover, the supercooled and glassy states lie between liquids and crystals, and thus the structures of the corresponding solutions may be a key in understanding the crystallization process of electrolyte solutions. In the past two decades Angell and his group[4] have made a systematic study of the characteristics of a large number of glassy solutions, i.e., glass-forming composition regions, glass transition temperatures, etc. With the exception of the work of Kanno and his co-workers,[5,6] there are relatively few reports of the study of equilibria between chemical species and their microscopic structures in the supercooled and glassy solutions.

We have started a comprehensive structural investigation of supercooled and glassy electrolyte solutions by X-ray and neutron diffraction and X-ray absorption spectroscopy and have reported the structures of several aqua metal ions in glassy electrolyte solutions.[7] In the present study such an investigation is extended to supercooled and glassy aqueous zinc(II) iodide solutions, in which the stepwise complex formation between zinc(II) and iodide ions takes place.

At ambient temperature comprehensive X-ray diffraction and Raman studies have been made for aqueous zinc(II) halide solutions. Wertz and Bell[8] performed X-ray scattering measurements on concentrated aqueous zinc(II) chloride–hydrochloric acid solutions with molar ratios $[Cl^-]/[Zn^{2+}]$ ranging from 2 to 6 and have concluded that the $[ZnCl_2(OH_2)_2]$ complex having the pseudotetrahedral structure is formed as a mean species in the solution with $[Cl^-]/[Zn^{2+}] = 2$. Several Raman measurements[9-13] on concentrated aqueous zinc(II) halide solutions have suggested the presence of tetrahedral species $[ZnX_n(OH_2)_{4-n}]^{(2-n)+}$ (X^- = halide ions) in the solutions. Johansson and his co-workers found, from X-ray and Raman measurements, that at ambient temperature the tetrahedral complexes, $[ZnX_2(OH_2)_2]$ and $[ZnX_3(OH_2)]^-$ ($X = Br^-, I^-$), are mainly formed in aqueous zinc(II) bromide[14] and iodide[15] solutions of 7.57 and 4.55 molar concentrations, respectively. From X-ray and Raman scattering experiments[16] on aqueous solutions of $ZnCl_2 \cdot RH_2O$ with $R = 1.8$ (saturated solution), 2.5, 3.0, 4.0, and 6.2, Yamaguchi et al. have concluded that the tetrahedral species $[ZnCl_n(OH_2)_{4-n}]^{(2-n)+}$ are predominantly formed in the solutions and that the average number of Zn–Cl interaction changes from ~2.4 for the solution of $R = 6.2$ to ~3.4 for the solution of $R = 1.8$.

For glassy aqueous zinc(II) halide solutions ($[H_2O]/[ZnX_2] = 10$) formed with quick vitrification, Kanno and Hiraishi[5] performed Raman spectroscopic measurements and identified chemical species present in the glassy solutions. According to their results the tetrahedral $[ZnX_4]^{2-}$ ions are the most stable ionic entities in the glassy state, and they have proposed the following equilibrium shifts to the right-hand side in the glassy state:

$$2ZnX_2 + 6H_2O \rightarrow ZnX_4^{2-} + Zn(OH_2)_6^{2+} \qquad (2)$$

In concentrated aqueous zinc(II) halide solutions at ambient temperature, however, the equilibrium shift (eq 2) hardly occurs as has been found from the X-ray and Raman studies stated above. Gilbert[17] has also noted that, at similar solute concentrations, the

* To whom correspondence should be addressed.
† On leave from Aqua Laboratory, Research and Development Division, TOTO Ltd., Nakashima, Kokurakita-ku, Kitakyushu 802, Japan.

(1) Burger, K. In *Solvation, Ionic and Complex Formation Reactions in Non-Aqueous Solutions*; Akadémiai Kiadó: Budapest, 1983; Chapter 5 and references cited therein.
(2) Franks, F. In *Water, A Comprehensive Treatise, Water and Aqueous Solutions at Subzero Temperatures*; Plenum Press: New York, 1982.
(3) Franks, F. In *Biophysics and Biochemistry at Low Temperatures*; Cambridge University Press: Cambridge, U.K., 1985.
(4) (a) Sare, E. J.; Angell, C. A. *J. Solution Chem.* **1973**, *2*, 53. (b) Angell, C. A.; Sare, E. J. *Cryo-Lett.* **1980**, *1*, 257.
(5) Kanno, H.; Hiraishi, J. *J. Raman Spectrosc.* **1980**, *9*, 85.
(6) (a) Kanno, H.; Hiraishi, J. *J. Raman Spectrosc.* **1982**, *12*, 224. (b) Kanno, H.; Hiraishi, J. *J. Phys. Chem.* **1983**, *87*, 3664. (c) Kanno, H. *J. Phys. Chem.* **1987**, *91*, 1967. (d) Kanno, H.; Shimada, K.; Katoh, K. *Chem. Phys. Lett.* **1983**, *103*, 219. (e) Kanno, H.; Shimada, K.; Yoshino, K.; Iwamoto, T. *Chem. Phys. Lett.* **1984**, *112*, 242.
(7) (a) Nomura, M.; Yamaguchi, T. *J. Phys., Colloq. C8* **1986**, *47* (Suppl. 12), 619. (b) Nomura, M.; Yamaguchi, T. *J. Phys. Chem.* **1988**, *92*, 6157. (c) Yamaguchi, T.; Nomura, M.; Wakita, H.; Ohtaki, H. *J. Chem. Phys.* **1988**, *89*, 5153. (d) Yamaguchi, T. *Pure Appl. Chem.* **1990**, *62*, 2251.
(8) (a) Wertz, D. L.; Bell, J. R. *J. Inorg. Nucl. Chem.* **1973**, *35*, 137; (b) **1973**, *35*, 861.
(9) Irish, D. E. In *Ionic Interactions*; Petrucci, S., Ed.; Academic Press: New York, 1971; Vol. II, pp 239–246.
(10) (a) Delwaulle, M. L. *C. R. Acad Sci.* **1955**, *240*, 2132. (b) Delwaulle, M. L. *Bull. Soc. Chim. Fr.* **1955**, 1294.
(11) Irish, D. E.; McCarroll, B.; Young, T. F. *J. Chem. Phys.* **1963**, *39*, 3426.
(12) Morris, D. F. C.; Short, E. L.; Slater, K. *Electrochim. Acta* **1963**, *8*, 289.
(13) Fontana, M. P.; Maisano, G.; Migliardo, P.; Wanderlingh, F. *J. Chem. Phys.* **1978**, *69*, 676.
(14) Goggin, P. L.; Johansson, G.; Maeda, M.; Wakita, H. *Acta Chem. Scand.* **1984**, *A38*, 625.
(15) Wakita, H.; Johansson, G.; Sandström, M.; Goggin, P. L.; Ohtaki, H. *J. Solution Chem.* **1991**, *20*, 643.
(16) Yamaguchi, T.; Hayashi, S.; Ohtaki, H. *J. Phys. Chem.* **1989**, *93*, 2620.
(17) Gilbert, B. *Bull. Soc. Chim. Belg.* **1967**, *76*, 493.

0022-3654/91/2095-10098$02.50/0

TABLE I: Compositions of the Sample Solutions [mol kg^{-1} (H_2O)]^a

	solution A	solution B
Zn^{2+}	10.88	5.555
I^-	21.75	11.11
ρ/g cm^{-3}	2.475	1.971
$V/10^8$ pm^3	2.760	4.206
$[H_2O]/[ZnI_2]$	5.103	9.993

^{a} V is the stoichiometric volume per Zn atom, and ρ is the density at 25 °C.

equilibrium constant is ca. 0.04. Thus, it is very interesting to examine whether equilibrium 2 takes place in the process of vitrification or in the supercooled solutions. Unfortunately, Kanno and Hiraishi did not measure Raman spectra of the corresponding supercooled solutions.

In the present investigation we have made Raman spectral measurements on both supercooled and glassy zinc(II) iodide solutions with different compositions and at various temperatures from ambient to liquid nitrogen temperatures. Furthermore, to determine an average structure of the chemical species in the corresponding solutions, X-ray diffraction measurements have also been performed on the same concentrated zinc(II) iodide solutions at room temperature and in the supercooled state. Finally, we discuss the chemical equilibrium in the supercooled and glassy solutions on the basis of the ion–ion, ion–water, and water–water interactions.

Experimental Section

Preparation of Sample Solutions. Sample solutions for X-ray diffraction and Raman measurements were prepared by dissolving zinc(II) iodide (Wako Pure Chemicals, 99.5%), which was used without further purification, in distilled water to reach $[H_2O]/[ZnI_2]$ molar ratios of 5 and 10. Concentrations of zinc(II) ion in the sample solutions were determined by direct titration with a standard EDTA solution using Eriochrome Black T (EBT) as an indicator. Densities of the solutions at 25 °C were determined pycnometrically, and those of the supercooled solutions were estimated by extrapolation of the densities of the zinc(II) iodide aqueous solutions in the temperature range from 5 to 100 °C in the literature[18] to supercooling temperatures. The compositions of the sample solutions are given in Table I.

Prior to the X-ray and Raman scattering measurements, the glass transition temperature of sample solution A was measured by differential scanning calorimetry (DSC) and found to be −96 °C. Thus, all the measurements at supercooling temperatures for solutions A and B were carried out above −80 °C.

X-ray Diffraction Measurements. X-ray diffraction measurements were carried out on a Rigaku θ–θ-type diffractometer using Mo Kα radiation (λ = 71.07 pm). A LiF crystal was used for monochromatization of scattered X-rays. The observed range of the scattering angle (2θ) was from 2° to 140°, corresponding to the scattering vector s ($=4\pi \sin\theta/\lambda$) of 3.1×10^{-3} to 0.166 pm^{-1}. The measurements were repeated twice over the whole angle range. Different slit combinations and step angles were used depending on the angle range, and a total amount of 80 000 counts was collected at each angle. Details of the X-ray measurements have been described elsewhere.[19,20] The measurements were performed at 25 and −5 °C for both solutions and at −20 °C only for solution A. Experiments below −20 °C were not possible because of crystallization of the solutions in a few hours. The temperatures of the sample solutions were measured with a copper–constantan thermocouple and controlled within ±0.2 °C by use of a cryostat (Figure 1) with a temperature control unit.

Raman Measurements. Each sample solution was sealed into a glass tube of 3-mm diameter. Raman spectra of the sample

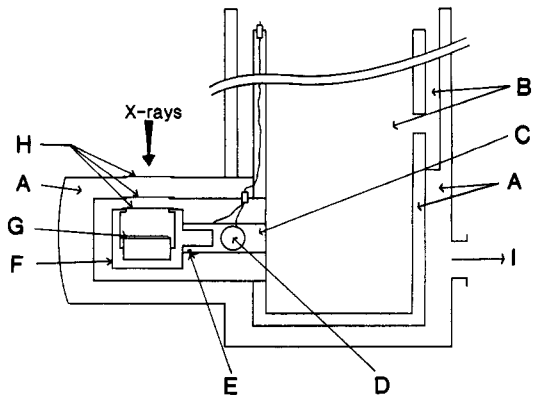

Figure 1. Schematic view of a cryostat used for X-ray measurements of the supercooled solutions: (A) vacuum jacket; (B) mixture of dry ice (solid carbon dioxide) and ethanol; (C) copper finger; (D) heaters; (E) copper–constantan thermocouple; (F) gold-coated sample holder; (G) Teflon sample cell; (H) Mylar film windows (200 μm in thickness); (I) to a vacuum pump.

solutions were recorded at 25, −5, −20, −40, −60, and −80 °C on a JEOL JRS-400T spectrometer. Raman spectra of the glassy solutions were measured by immersing the sample tube into liquid nitrogen (−196 °C). The 514.5-nm line radiated from an argon ion laser (Spectra Physics Model 168B) was used for all measurements.

X-ray Data Treatment. Corrections for background, absorption, polarization, and multiple scattering of X-rays to the observed intensities were made in the usual way.[21] The structure functions $i(s)$ are given by

$$i(s) = KI(s) - \sum_j n_j f_j^2(s) \quad (3)$$

where K represents a normalization factor of the observed intensities $I(s)$ to absolute units, n_j is the number of atom j in a stoichiometric volume V containing one Zn atom, and $f_j(s)$ is the atomic scattering factor of atom j corrected for the anomalous dispersion. The structure functions of the sample solutions, multiplied by s, are shown in Figure 2. The $si(s)$ values are Fourier transformed into the radial distribution function $D(r)$ as

$$D(r) = 4\pi r^2\rho_0 + (2r/\pi)\int_0^{s_{max}} si(s)M(s) \sin(rs)\, ds \quad (4)$$

Here, ρ_0 ($=[\sum n_j f_j(0)]^2/V$) stands for the average scattering density of the sample solution and s_{max} is the maximum s value attained in the measurements (s_{max} = 0.166 pm^{-1}). The modification function $M(s)$ has the form

$$M(s) = [\sum n_j f_j^2(0)/\sum n_j f_j^2(s)] \exp(-ks^2) \quad (5)$$

with the damping factor k being chosen as 100 pm^2 in the present case.

A comparison between the experimental and theoretical structure functions was made by a least-squares refinement procedure of minimizing the error square sum:

$$U = \sum_{s_{min}}^{s_{max}} s^2[i(s)_{obsd} - i(s)_{calcd}]^2 \quad (6)$$

The theoretical intensities $i(s)_{calcd}$ were calculated by the following equation:

$$i(s)_{calcd} = \sum\sum_{\substack{pq \\ p\neq q}} n_{pq} f_p(s) f_q(s) \frac{\sin(r_{pq}s)}{r_{pq}s} \exp(-b_{pq}s^2) - \sum\sum_{\substack{pq \\ p\neq q}} n_p n_q f_p(s) f_q(s) \frac{4\pi R_q^3}{V} \frac{\sin(R_q s) - R_q s \cos(R_q s)}{(R_q s)^3} \exp(-B_q s^2) \quad (7)$$

The first term of the right-hand-side of eq 7 is related to the

(18) Söhnel, O.; Novotný, P. In *Physical Sciences Data 22, Densities of Aqueous Solutions of Inorganic Substances*; Elsevier: New York, 1985.
(19) Wakita, H.; Ichihasi, M.; Mibuchi, T.; Masuda, I. *Bull. Chem. Soc. Jpn.* **1982**, *55*, 817.
(20) Yamaguchi, T.; Johansson, G.; Holmgerg, B.; Maeda, M.; Ohtaki, H. *Acta Chem. Scand.* **1984**, *A38*, 437.
(21) Johansson, G.; Sandström, M. *Chem. Scr.* **1973**, *4*, 195.

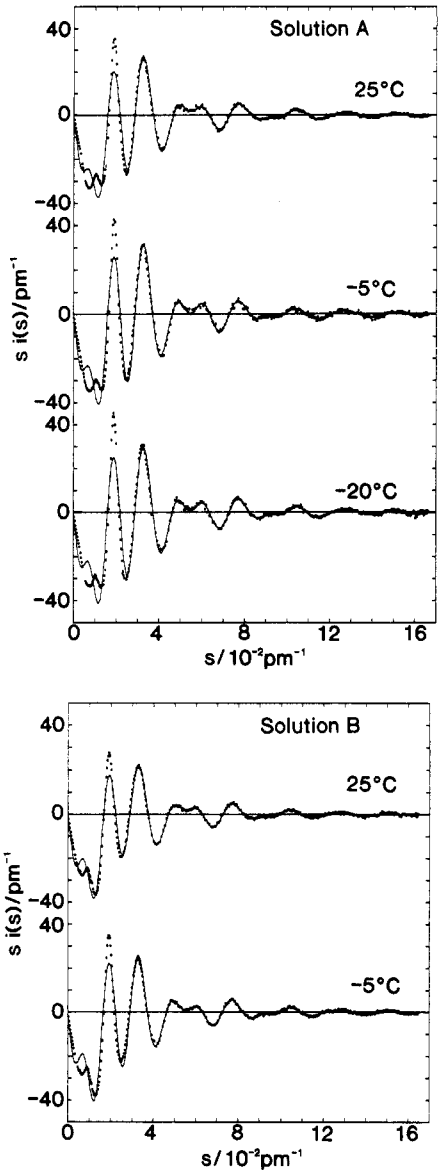

Figure 2. Structure functions $i(s)$ multiplied by s of the concentrated zinc(II) iodide solutions at various temperatures. The experimental values are drawn by dots and those calculated with the parameter values given in Tables II and III by solid lines. Solution A is shown at 25, -5, and -20 °C and solution B at 25 and -5 °C.

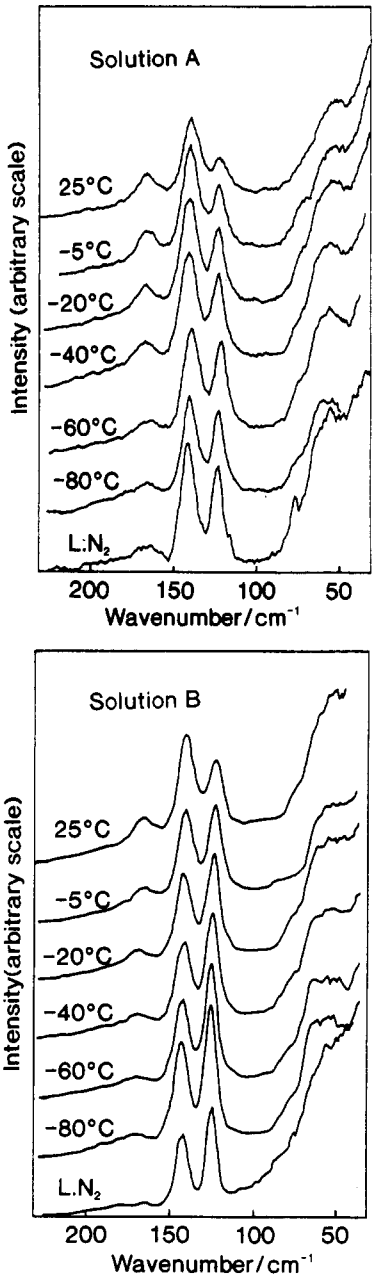

Figure 3. Raman spectra of the concentrated aqueous zinc(II) iodide solutions A and B at various temperatures. The spectrum at liquid nitrogen temperature corresponds to the glassy solution.

short-range interactions characterized by the interatomic distances r_{pq}, the temperature factor b_{pq}, and the number of interactions n_{pq} for atom pair p–q. The second term arises from the interaction between a spherical hole and the continuum electron distribution beyond this discrete distance. R_p is the radius of the spherical hole around the qth atom and B_q the softness parameter for emergence of the continuum electron distribution.

Programs KURVLR[21] and NLPLSQ[22] were used for all calculations of the X-ray data.

Results

Raman Spectra. Raman spectra of solutions A and B at various temperatures are shown in Figure 3. The spectral patterns of solution B at 25 °C and liquid nitrogen temperature are in good agreement with those reported by Kanno and Hiraishi.[5] The intense Raman bands are observed at 165, 139, and 122 cm^{-1} for both solutions, which are assigned to the ν_1 mode of the totally symmetric Zn–I vibration within the diiodo-, triiodo-, and tetraiodozinc(II) complexes, respectively. Kanno and Hiraishi observed a drastic increase in intensity of the ν_1 band of the tetraiodo complex when an aqueous solution of $ZnI_2 \cdot 10H_2O$ was quickly vitrified from liquid at room temperature to glassy state at liquid nitrogen temperature. As seen in Figure 3, however, such an intensity change of the ν_1 band occurs even at -5 °C in the supercooled solutions. With decreasing temperature the intensity of the band at 122 cm^{-1} for the tetraiodo complex gradually increases and appears to be constant below -40 °C. A larger change in intensity of the band is observed for water-rich solution B than for solution A. On the other hand, the ν_1 band of the diiodozinc(II) complex decreases in intensity with temperature and almost disappears below -60 °C for solution B. The ν_1 band of the triiodo complex does not change significantly with temperature. Thus, in the supercooled solutions as well as the glassy state the diiodo complex is less favored and the tetraiodo species is more stabilized.

Figure 4 shows a broad Raman band around 390 cm^{-1} at various temperatures; the band is ascribed to the totally symmetric Zn–O vibration for the aqua zinc(II) ion according to Raman spectral measurements of a 3.36 mol kg^{-1} aqueous zinc(II) nitrate solution by Bulmer et al.[23] Interestingly, the intensity of the ν_1 band of

(22) Yamaguchi, T. Doctoral Thesis, Tokyo Institute of Technology, 1978.

(23) Bulmer, J. T.; Irish, D. E.; Ödberg, L. *Can. J. Chem.* **1975**, *53*, 3806.

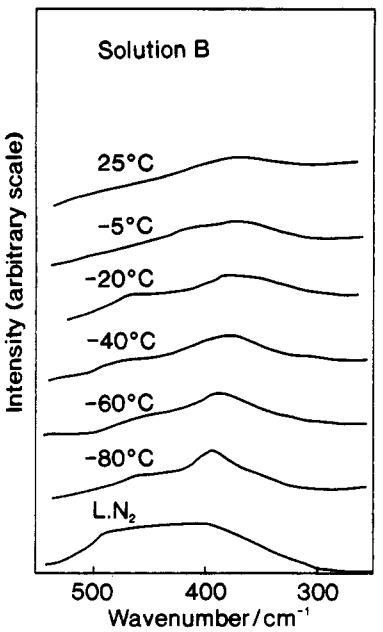

Figure 4. Raman spectra of concentrated aqueous zinc(II) iodide solution B at various temperatures. The spectrum at liquid nitrogen temperature corresponds to the glassy solution.

the aqua complex increases with lowering temperature, indicating that the aqua zinc(II) ions, the lowest species in a series of the zinc(II) iodo complexes, are also favored in the supercooled and glassy solutions. The peak position shifts to higher wavenumbers with decreasing temperature. Bulmer et al.[23] have also observed a similar shift for the aqueous zinc(II) nitrate solution over the temperature range from 80 to -29 °C and stated that the shift arises from the change of the contribution of hot band excitation with temperature. Furthermore, this Raman band for the glassay state shows the broader contour from 400 to 500 cm^{-1}, which is ascribed to the libration mode of water molecules. Similar spectra have also been observed in the spectra for glassy aqueous solutions of lithium halides and calcium halides.[24]

X-ray Radial Distribution Functions (RDFs). The total RDFs in the form of $D(r) - 4\pi r^2\rho_0$ for solutions A and B are shown in Figure 5. Since the present sample solutions contain heavy iodine and zinc atoms, the total RDFs arise mainly from the interactions related to iodide and zinc(II) ions. In all RDFs two predominant peaks are observed at 258 and 430 pm. A broad peak appears at 600–900 pm, which originates from various long-range interactions in the solutions. Since the long-range interactions are too complicated to be uniquely determined, the broad peak was not analyzed in the present work. The first peak is assigned to the Zn–I bonds within various zinc(II) iodo complexes present in the solutions. The second peak is expected to be due mainly to nonbonding I···I interactions within the tetrahedral zinc(II) iodo complexes, because the ratio (1.67) of the I···I to the Zn–I peak positions is close to 1.63, an expected value $[(8/3)^{1/2}]$ for a tetrahedral coordination. The nonbonding O(H_2O)···I interactions within the tetrahedral diiodo and triiodo species, $[ZnI_2(OH_2)_2]$ and $[ZnI_3(OH_2)]^-$, in equilibrium may also contribute to the peak at about 383 pm. In addition, the interactions between the ligand atoms within the zinc(II) complexes and the ions and/or water molecules in the second shell will also fall within 350–550 pm according to the crystal structure of $ZnI_3{\cdot}2H_2O$.[25]

When temperature is lowered, the first Zn–I peak does not change significantly, but the second peak becomes progressively larger and sharper for both solutions. It should be noted that a very small peak can be observed around 210 pm in the RDFs of the supercooled solutions. This peak may be attributed to the Zn–O interactions within the aqua zinc(II) ion as suggested from the Raman spectra of the supercooled solution B.

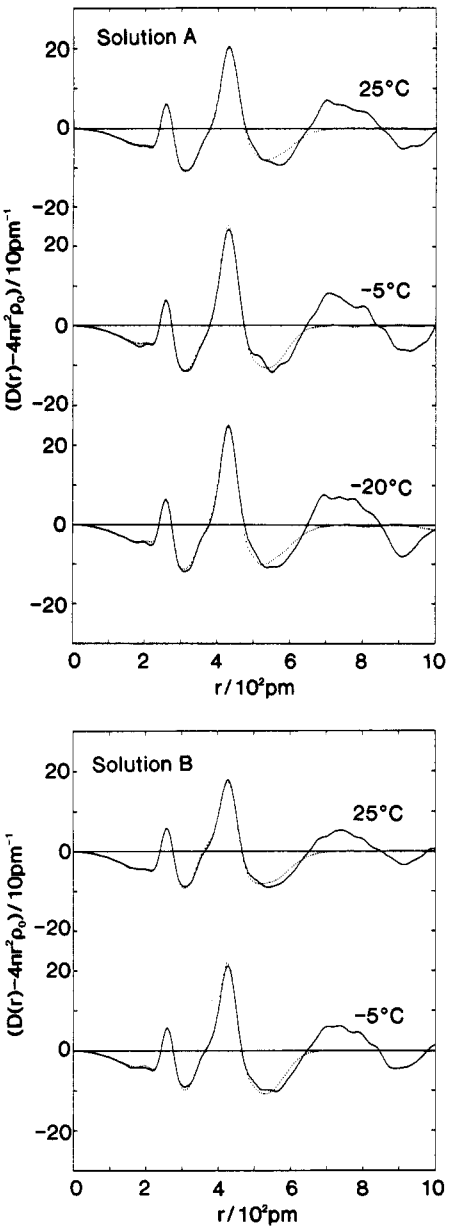

Figure 5. Radial distribution functions in the form of $D(r) - 4\pi r^2\rho_0$ of the concentrated zinc(II) iodide solutions at various temperatures: (solid lines) experimental and calculated (dotted lines). Solution A is shown at 25, -5, and -20 °C and solution B at 25 and -5 °C.

To perform a quantitative analysis of the X-ray diffraction data, the least-squares method was applied to the structure functions over the scattering vector range of $0.1 \times 10^{-2} < s/pm^{-1} < 0.166$ with the interatomic distance r, the temperature factor b, the number of interactions n, and the parameters R and B for a continuum electron distribution as variables. All interactions discussed above were included in the calculations. The optimized parameter values for solutions A and B are summarized in Tables II and III. Those for the glassy state obtained from previous extended X-ray absorption fine structure investigations[26] are also included for comparison. Figure 5 shows that theoretical RDFs calculated by using the optimized parameters reproduce well the observed ones except the region of the long-range interactions not taken into account in Tables II and III. The Zn–I and I–I distances (259 and 430 pm, respectively) obtained for both solutions show little change with temperature and are in good agreement with the values reported for X-ray diffraction studies of aqueous zinc(II) iodide solutions at ambient temperature.[15] An average coordination number of iodide ions for a zinc(II) ion (n_{Zn-I}) is

(24) Kanno, H.; Hiraishi, J. *Chem. Phys. Lett.* **1980**, *72*, 541.
(25) Holinski, von R.; Brehler, B. *Acta Crystallogr.* **1970**, *B26*, 1915.
(26) Yamaguchi, T.; Kamihata, K.; Wakita, H.; Nomura, M. Photon Factory Activity Report. National Laboratory for High Energy Physics, KEK-PF, Tsukuba, 1988; Vol. 6, p 45.

TABLE II: Optimized Parameter Values of the Interactions within the Zinc(II) Iodide Complexes at Various Temperatures

interaction	parameter	solution A			solution B		glass[a] liquid N_2
		25 °C	−5 °C	−20 °C	25 °C	−20 °C	
Zn–O	r	210	210	210	204 (1)	203 (1)	
	$b/10$	3	3	3	3	3	
	n	2.59	2.70	3.00	2.3 (3)	3.3 (3)	
Zn–I	r	257.9 (2)	258.4 (3)	259.0 (3)	258.5 (2)	259.3 (2)	259
	$b/10$	2.5	2.5	2.5	5	5	
	n	1.96 (2)	2.06 (4)	2.06 (4)	1.92 (2)	2.01 (4)	2.0
I···I	r	430.1 (3)	428.5 (4)	430.1 (4)	429.4 (4)	428.1 (4)	
	$b/10$	16	16	16	25	25	
	n	2.07 (3)	2.36 (5)	2.50 (5)	1.98 (4)	2.33 (4)	
I···O	r	383	383	383	383	383	
	$b/10$	10	10	10	10	10	
	n	2.43	1.75	1.75	2.43	1.75	

[a] Reference 13. Interatomic distance r (pm), temperature factor b (pm^2), and number of interactions n. The values in parentheses are standard deviations of the last figure. The parameters without standard deviations were not allowed to vary in the calculations.

TABLE III: Optimized Parameter Values of the Medium-Range Interactions and of the Continuum Electron Distribution at Various Temperatures

interaction	parameter[a]	solution A			solution B	
		25 °C	−5 °C	−20 °C	25 °C	−20 °C
Zn···O	r	410	409	400	409	399
	$b/10$	22	17	22	10	20
	n	14	15	13	4	4.4
I–O	r	356	360	357	357	354
	$b/10$	9	15	10	14	15
	n	4	6	5	5.6	6
Zn···H_2O	r	542	535	546	521	526
	$b/10$	20	20	20	20	20
	n	4	5	6	5	2
I–O	r	453	450	445	432	427
	$b/10$	10	12	21	10	10
	n	5	8	8	5	7
I···O	r	491	495	492	487	491
	$b/10$	17	20	14	10	20
	n	5	5	5	2	4
Zn	R	273 (9)	303 (9)	296 (11)	218 (10)	263 (11)
	$B/10$	10	10	10	10	10
I	R	548 (2)	561 (2)	561 (2)	551 (1)	559 (2)
	$B/10$	173 (17)	92 (15)	132 (18)	158 (14)	92 (13)
H_2O	R	363 (5)	415 (5)	385 (6)	329 (2)	355 (3)
	$B/10$	10	10	10	38	81

[a] Interatomic distance r (pm), temperature factor b (pm^2), and number of interactions n. The values in parentheses are standard deviations of the last figure. The parameters without standard deviations were not allowed to vary in the calculations.

2.0 in the room temperature and the supercooled solutions and thus practically independent of temperature. The number of I···I interactions, however, increases from 2.07(3) at 25 °C to 2.50(5) at −20 °C for solution A and from 1.98(4) at 25 °C to 2.33(4) at −5 °C for solution B. The increase in n_{I-I} of 0.4 is beyond estimated uncertainties in the X-ray analysis, and hence the present results suggest that the formation of the higher zinc(II) iodo complexes like the tetraiodo species is more favored at the supercooled state than at the ambient temperature. The increase in the number of Zn–O interactions in solution B, from 2.3(3) at 25 °C to 3.3(3) at −5 °C, indicates preferred formation of aqua zinc(II) species at the supercooled state. These findings are consistent with the results from the Raman spectra shown in the previous section.

Discussion

The present X-ray diffraction and Raman spectroscopic studies have demonstrated that the highest complex, $[ZnI_4]^{2-}$, and the aqua zinc(II) ion, $[Zn(OH_2)_6]^{2+}$, as well as the triiodozinc(II) complex are preferentially formed, while the diiodozinc(II) complex, $[ZnI_2(OH_2)_2]$, is unstable in the supercooled solutions as well as in the glassy state. Thus, we conclude that the equilibrium shift (eq 1) to the right-hand side is not caused by the quick vitrification process of the solutions.

Additionally, as seen in Figure 3, the formation of the tetraiodo species is more promoted for solution B than for solution A. This result suggests the equilibrium shift (eq 1) is more favored with increasing water content.

On the basis of the above findings we now discuss possible reasons for this equilibrium shift. Previous structural[15] and thermodynamic[27] data for an aqueous zinc(II) iodide solution at ambient temperature have suggested that the structural transformation of the zinc(II) iodo complexes from octahedral to tetrahedral takes place at the second step where the diiodo complex is formed. Thus, in the formation of the triiodo and tetraiodo complexes one water molecule within the first coordination shell of the diiodo and the triiodo species is replaced stepwise with one iodide ion. The stepwise enthalpies, ΔH_n, of the zinc(II) iodo complexes at ambient temperature are positive for n = 1–3 but negative for n = 4.[28] Since the energy gained from one Zn–I bond formation at n = 3 and 4 may be similar at each step of complex formation, the different signs of ΔH_n for n = 3 and 4 may be ascribed to an energy difference in breaking one Zn–OH_2 bond within the diiodo and triiodo complexes. The negative value of ΔH_4 indicates less energy required to break one Zn–OH_2 bond within the triiodo complex, compared with the case of the diiodo complex. This expectation may hold in the solution at a constant temperature since the ion–water and water–water interactions do not differ appreciably in the solution. However, when temperature is lowered, in particular below the melting point of water, the magnitude of the ion–water and water–water interactions will

(27) Ahrland, S.; Kullberg, L.; Portanova, R. *Acta Chem. Scand. Ser. A* **1978**, 251.

(28) Sillén, L. G.; Martell, A. E. In *Stability Constants of Metal-Ion Complexes*; Special Publication 17; The Chemical Society: London, 1964.

change greatly, although the ion-ion interaction itself may be similar in solutions at room temperature and at supercooled and glassy states. Our X-ray and neutron diffraction studies[29] on supercooled and glassy aqueous solutions of $LiCl \cdot 5H_2O$ and $LiCl \cdot 5D_2O$, respectively, have shown that the hydrogen-bonded network of water molecules is enhanced up to the third nearest neighbors.[30] If this is the case in the present supercooled and glassy zinc(II) iodide solutions, water molecules dispelled from the first coordination shell of the diiodozinc(II) complex will be stabilized in the strengthened hydrogen bond framework, and consequently iodide ions will more easily bind to the zinc(II) ion to form the tetraiodo complex. In the case of the triiodozinc(II) complex present in solutions at room temperature and supercooled and glassy states, a water molecule within the coordination shell may be weakly bound to the zinc(II) ion and is thus not affected by the enhancement of hydrogen bonds in the supercooled and glassy solutions. When the tetraiodo zinc(II) species increases in the supercooled and glassy solutions, the aqua zinc(II) ions will be formed in a water-rich region to satisfy the stoichiometry of the solute.

Here, it is interesting to note the results of Raman measurements for aqueous zinc(II) bromide solutions from 25 to 300 °C by Yang et al.[31] that the formation of monobromo- and dibromozinc(II) complexes increases with increasing temperature. In aqueous solution at the higher temperatures, in which the hydrogen-bonded network is less significant, the lower halogeno zinc(II) complexes are favored. Thus, water does play an important role in the formation of the zinc(II) halogeno complexes in aqueous solution at various temperatures.

In summary, in supercooled and glassy aqueous solutions in the presence of complex-forming ions, the equilibrium of labile species is greatly affected by strengthened water-water interactions and thus quite different from that in the corresponding solution at ambient temperature. This fact is very important to consider in investigations of chemical reactions, coordination species, etc. in supercooled and glassy aqueous solutions. This equilibrium shift in the supercooled and glassy solutions will become a key to clarify freezing and crystallization of the aqueous electrolyte solutions.

Acknowledgment. We thank Mr. Kazumasa Yoshikai for his help in the Raman spectral measurements. The present work was partially supported by a Grant-in-Aid for Scientific Research on Priority Area of "Molecular Approahes to Non-equilibrium Processes in Solutions" (2245106) from the Ministry of Education, Science and Culture, Japan. All of the calculations were performed at the Computer Center of Fukuoka University.

(29) Yamaguchi, T.; Yamagami, M.; Kurisaki, T.; Takamuku, T.; Wakita, H. Unpublished data.

(30) In the present RDFs of the zinc(II) iodide aqueous solutions, the corresponding second and third neighbor H_2O–H_2O peaks, which have appeared at 450 and 690 pm, respectively, for liquid water, are not discernible because of the presence of the dominant Zn- and I-related peaks.

(31) Yang, M. M.; Crerar, D. A.; Irish, D. E. *J. Solution Chem.* **1988**, *17*, 751.

High-Pressure Raman Scattering and Inelastic Neutron Scattering Studies of Triaminotrinitrobenzene

Sushil K. Satija,† Basil Swanson,* Juergen Eckert,* and J. A. Goldstone

Los Alamos National Laboratory, University of California, Los Alamos, New Mexico 87545
(Received: May 15, 1991)

We report the results of the effect of static pressure on the Raman spectrum of TATB up to pressures of 160 kbar and deuterated TATB (DTATB) up to pressures of 65 kbar. Both these solids are found to be remarkably stable to high densities. We observe unusual pressure dependence of the δ_{NO_2}, ν_{C-N}, and ν_{N-O} modes and attribute these changes to variation in NH_2/NO_2 coupling as the pressure is increased. Both of these aspects of TATB may be important in contributing to the insensitivity of TATB to shock-initiated detonation. We also find that, unlike at ambient pressures, TATB is quite insensitive to photolysis when exposed to static pressures exceeding 15 kbar, indicating that photolysis of TATB involves a positive activation volume. In addition, we present inelastic neutron scattering data as well as some assignments of TATB and two related substituted anilines, *p*-nitroaniline and *p*-chloroaniline. These clearly demonstrate the strong vibrational coupling between NH_2 and NO_2 groups.

Introduction

There is considerable interest in understanding the detonation of high explosives (HE's) at a microscopic level. One of the recent advances in high-explosive technology is the development of materials such as triaminotrinitrobenzene (TATB)[1] which are remarkably insensitive to shock initiation, offering a considerable improvement in safety in contrast to conventional HE's which are susceptible to accidental detonation.

Several models have been proposed to explain the behavior of insensitive high explosives (IHE's).[2] At this time, however, there is no model which can be applied to the wide range of known IHE's. The present report on the behavior of TATB to static high-pressure conditions is part of an ongoing effort to understand what controls the chemical transformations which accompany shock propagation and, in particular, shock initiation of HE's.

One aspect of detonation phenomena which has long been of interest is how energy is transferred from the mechanical forces in shock wave to be localized in bonds leading to the early chemical transformations associated with shock initiation. One view is that macroscopic phenomena dominate shock initiation and that energy is thermalized rapidly, resulting in equilibrium thermodynamics and chemistry which is predictable on the basis of known high-temperature behavior. This perspective allows for the existence of hot spots[3] in shock propagation through condensed-phase materials resulting in inhomogeneities in the bulk materials and

* To whom correspondence should be addressed.
† Present address: Reactor Radiation Division, National Institute of Standards and Technology, Gaithersburg, MD 20899.

(1) Ayers, J. N.; Montesi, L. J.; Bauer, R. J. NOLTR 73-132, Naval Ordinance Laboratory, White Oak, Silver Springs, MD, 1973.

(2) See: Lee, E. L.; Tarver, C. M. *Phys. Fluids* **1980**, *23*, 2362, and references therein for phenomenological models.

(3) Campbell, A. W.; Davis, W. C.; Ramsey, J. B.; Travis, J. R. *Phys. Fluids* **1961**, *4*, 511.

0022-3654/91/2095-10103$02.50/0